Available online at www.sciencedirect.com
SCIENCE DIRECT®
Journal of Catalysis 222 (2004) 268–280
JOURNAL OF CATALYSIS
www.elsevier.com/locate/jcat

In situ EXAFS study on the oxidation state of Pd/Al_2O_3 and $Bi–Pd/Al_2O_3$ during the liquid-phase oxidation of 1-phenylethanol

Csilla Keresszegi, Jan-Dierk Grunwaldt, Tamas Mallat, and Alfons Baiker *

Institute for Chemical and Bioengineering, Swiss Federal Institute of Technology, ETH Hönggerberg HCI, CH-8093 Zurich, Switzerland

Received 31 July 2003; revised 8 October 2003; accepted 21 October 2003

Abstract

In situ XANES and EXAFS were used to uncover the oxidation state of the metal constituents in a 5 wt% Pd/Al_2O_3 and a 0.75 wt% Bi–5 wt% Pd/Al_2O_3 catalyst during the liquid-phase dehydrogenation and oxidation of 1-phenylethanol. The catalytic reactions were carried out in a continuous-flow fixed-bed reactor serving at the same time as a spectroscopic cell for XANES/EXAFS. A special technique was applied to deposit Bi mainly as adatoms onto the supported Pd particles, as evidenced by XPS and XAS. Due to this technique, most Bi atoms were located on the Pd surface and thus the Bi dispersion was higher than that of Pd. This feature of the bimetallic catalysts led to more pronounced changes in the XANES region at the Bi L_3- than at the Pd K-edge. As a result, the method was more surface sensitive to the minor component Bi than to the major component Pd. The studies revealed that both the active sites (Pd) and the promoter (Bi) were in a metallic state during dehydrogenation in He. After the introduction of molecular oxygen the metals remained in a reduced state as long as the oxygen supply was limiting the global reaction rate, indicating a dehydrogenation mechanism of alcohol oxidation. As soon as the rate of oxygen supply exceeded the rate of alcohol dehydrogenation, both Bi and Pd were successively oxidized, leading to the well-known "overoxidation" (deactivation) phenomenon. An important consequence of the observations to the reaction mechanism is that the promoter effect of Bi cannot be related to its (partially) oxidized state (Bi^{n+}), or to Bi leaching and homogeneous catalysis.

Keywords: In situ EXAFS; XANES; Alcohol oxidation; Alcohol dehydrogenation; 1-Phenylethanol; Palladium; Bismuth; Promoter; Oxidation state; Reaction mechanism

1. Introduction

Oxidation of alcohols to the corresponding carbonyl compounds and carboxylic acids over supported noble metal catalysts is an attractive "green" technology: molecular oxygen can be used as oxidant and the coproduct is water [1–9]. In the past years, various sophisticated bi- and multimetallic catalysts have been developed. The mostly used catalysts consist of Pt or Pd as active components, and Bi, Pb, or Te as promoter. The promoter alone is inactive under reaction conditions but can dramatically enhance the reaction rate [10,11] and selectivity [12,13].

Numerous models have been proposed to interpret the role of promoters:

(i) According to a popular model, the selectivity enhancement is due to a complex formation between an α-functionalized alcohol, a surface Pt or Pd atom, and a positively charged promoter atom or promoter ion [2,14,15].
(ii) Geometric blocking of a fraction of active sites may be responsible for the rate acceleration [16,17]. This so called "ensemble effect" is traced back to the bigger active site ensembles necessary for the formation of poisoning intermediates (by, e.g. C–C bond cleavage), compared to the site requirement of the alcohol dehydrogenation reaction.
(iii) The rate acceleration may be attributed to bifunctional catalysis, assuming that oxygen or OH radicals adsorbed on the promoter atom are involved in alcohol oxidation [18,19].
(iv) For a similar reason, Bi may act as a cocatalyst due to its higher affinity for oxygen and protect Pt or Pd

* Corresponding author.
E-mail address: baiker@tech.chem.ethz.ch (A. Baiker).

0021-9517/$ – see front matter
doi:10.1016/j.jcat.2003.10.013

from overoxidation [15]. That is, during reaction Bi would be in a higher oxidized state than the noble metal.

(v) The improved catalytic performance might be attributed to the formation of an ordered alloy (intermetallic compound) between the active component (Pt or Pd) and the promoter atom (Bi or Te) [20–22].

(vi) Finally, leaching of Bi as Bi^{3+} and the possible role of homogeneous complexes have also been thoroughly investigated [23].

We assume that the major reason for the obvious disagreement lies in the difficulties in investigating the location and oxidation state of the promoter during alcohol oxidation. The possibilities of using in situ techniques for studying the solid/liquid interphase in catalysis are limited. Infrared spectroscopy can give only indirect and qualitative information on the oxidation state but is well suited for the study of adsorbates [24–26]. An electrochemical method, the measurement of catalyst potential during reaction [27–29], is restricted to conductive, usually aqueous media. In addition, it provides only an indirect information on the oxidation state of promoter as the measured value ("mixed potential" [30, 31]) is influenced by various surface species, and strong adsorption of by-products on the collector electrode can distort the results [11].

Extended X-ray absorption fine structure (EXAFS) spectroscopy has been used for direct structural characterization of the working catalyst in gas/solid-type reactions [32–37]. Dynamic changes in the catalyst structure can be monitored by applying dispersive EXAFS (DEXAFS) or quick EXAFS (QEXAFS) [32,38–41]. It is also a powerful tool for in situ characterization of the solid/liquid interphase [8,42,43], including the aqueous alcohol oxidation reaction over Pt [44]. Recently, we have shown that dynamic changes can be monitored in situ during alcohol oxidation on Pd/Al_2O_3 by EXAFS and QEXAFS techniques using a continuous-flow fixed-bed reactor as the EXAFS cell [45].

An interesting challenge is the extension of the application range of the method to bimetallic catalysts and the clarification of the oxidation state of the promoter metal. One of the limitations is that XAS is a bulk technique. Here we show that the surface sensitivity can be enhanced by depositing the promoter metal onto the surface of the supported Pd catalyst. Dehydrogenation and oxidative dehydrogenation of 1-phenylethanol in toluene have been chosen as model reactions for the in situ EXAFS study of $Bi–Pd/Al_2O_3$ and Pd/Al_2O_3 catalysts. Some preliminary results have been reported in a recent communication [46]. A special effort is made to reveal a potential correlation between the oxidation state and the effect of the Bi promoter on the catalytic behavior of the palladium catalyst.

2. Experimental

2.1. Materials

1-Phenylethanol (Aldrich, 98%), toluene (J.T. Baker, $>99.5\%$), cyclohexane (Aldrich, 99+%), and water (Merck, 100%) were used as received. Gases were of 99.999% purity. The 5 wt% Pd/Al_2O_3 catalyst (Johnson Matthey 324; surface average diameter: 3.4 nm determined by TEM; calculated metal dispersion: 0.34 [47]) was used as received.

The bimetallic catalyst 0.75 wt% Bi–5 wt% Pd/Al_2O_3 was prepared by the preferential deposition of promoter metal adatoms onto the surface of Pd particles [19,48,49]. At first, 2.5 g 5 wt% Pd/Al_2O_3 was prereduced by hydrogen in 200 ml water at room temperature. After 20 min the pH was set to 3 with 3 ml acetic acid and 49.3 mg $Bi(NO_3)_3 \cdot 5H_2O$ (Fluka, $>99\%$) dissolved in 80 ml 2% aqueous acetic acid was dropped to the stirred slurry in 30 min in a hydrogen atmosphere. After 5 min, 3 ml 2-propanol (J.T. Baker, $>99.5\%$) was added in order to keep the metals in a reduced state during filtration. The system was flushed with nitrogen, the catalyst was filtered off, washed to neutral with 1% aqueous 2-propanol solution, then suspended with 0.05 M $NaHCO_3$ solution, and washed again with water to neutral. The catalyst was dried under vacuum at room temperature. The Bi content of the catalyst was calculated from the edge jump of a XANES spectrum.

2.2. Catalytic studies in a slurry reactor

Oxidation and dehydrogenation of 1-phenylethanol was carried out in a flat-bottomed, magnetically stirred 150 ml glass reactor. In a typical reaction, 0.10 g catalyst, 1.0 g alcohol, and 30 ml solvent were stirred at 55–80 °C and 1 bar, in Ar or air.

2.3. Catalytic studies in the EXAFS cell

The measurements were carried out at the Hamburger Synchrotron Laboratory (HASYLAB at Deutsches Elektronensynchrotron (DESY), Hamburg, Germany) in a continuous-flow reactor cell (0.12 ml), which allowed simultaneous catalytic and structural studies. A similar setup has been described previously [45]. A closed system was used where all gas-out lines were connected to the exhaust system. Powdered catalyst was applied and the dead volume was minimized to improve the flow characteristics. The reactor cell was filled with 28 mg catalyst. The reaction mixture (20.5 mM 1-phenylethanol in toluene) was stored in two separate glass bubble tanks [25], where the liquid could be saturated with He or O_2 at 1 bar. The third tank contained pure toluene saturated with He, O_2, or H_2. Liquids were provided from the tanks to the reactor or through a bypass to the purging collector vessel by a peristaltic pump (ISMATEC Reglo 100) put in front of the reactor. The flow rate was 0.68 ml min^{-1} except for oxygen-saturated toluene

(1.19 ml min^{-1}). The joints and tubes transferring oxygen-free medium were made of stainless steel in order to avoid oxygen diffusion into the feed. Samples were taken periodically for GC analysis (Thermo Quest Trace 2000, equipped with an HP-FFAP capillary column and an FID detector). Products were identified by GC-MS, and by GC analysis of authentic samples. Under the conditions applied steady state was reached within 15 min and the conversion and selectivity could be reproduced within ± 0.1 and $\pm 0.5\%$, respectively.

The reactor, located in an oven, was fixed on an x, z, θ table to allow positioning of the cell in the beam. The X-rays passed through the reactor cell via X-ray transmitting windows (such as Al foil, Kapton). Typically, QEXAFS spectra were taken when structural changes were expected and EXAFS spectra were recorded only after reaching steady state conditions.

2.4. X-ray absorption spectroscopy (EXAFS, XANES, QEXAFS)

Experiments were performed at beamline X1 at the DORIS III ring at DESY (ring operating at 4.4 GeV, injection current 140 mA) in the transmission geometry using Si(311) and Si(111) double crystals for monochromatization of the beam at the Pd K- and Bi L_3-edges, respectively. By detuning the crystals to 70% of the maximum intensity, higher harmonics were effectively eliminated. Three ionization chambers filled with Ar were used to record the intensity of the incident and the transmitted X-rays. For the Bi L_3-edge a more appropriate ionization chamber mixture of Ar/N_2 was only used for ex situ and reference catalyst scans, since changes of gasses would decelerate the speed of measurement on the *same* catalyst at the Bi L_3- and the Pd K-edges. In contrast, monochromator crystal change can be achieved within a few minutes. The cell was located between the first and second chamber. The reference foils for energy calibration were placed between the second and the third ionization chamber (Pd or Ag for Pd K-edge and Bi or Au for Bi L_3-edge). In the case of Pd, EXAFS spectra were taken around the Pd K-edge in the step scanning mode between 24,000 and 25,600 eV. Quick EXAFS (QEXAFS) scans were recorded in the continuous scanning mode between 24,300 and 24,800 eV (typically 80 s/scan). EXAFS spectra around the Bi L_3-edge were recorded between 13,350 and 14,400 eV, and QEXAFS scans between 13,400 and 13,580 eV (typically 70 s/scan). The raw data were energy-calibrated with the respective metal foil, background-corrected, normalized, and fitted using the WINXAS 2.1 package [50]. For EXAFS data analysis, Fourier transformation was applied on the k^3-weighted functions in the interval $k = 3.5$–16 Å^{-1} for Pd. For QEXAFS data around the Pd K-edge an interval $k = 2.8$–10.5 Å^{-1} was chosen. During reduction and oxidation of the Pd and Bi constituents, the extent of reduction or oxidation was calculated by a linear combination of the starting and end spectra or appropriate reference data. The procedure is described in the results part.

2.5. X-ray photoelectron spectroscopy (XPS)

The XPS analysis of the Pd/Al_2O_3 and $Bi–Pd/Al_2O_3$ catalysts was performed on a Leybold Heraeus LHS11 MCD instrument using Mg K_α (1253.6 eV) radiation. The sample was pressed into a sample holder, evacuated in a load lock to 10^{-6} mbar, and transferred to the analysis chamber (typical pressure $< 10^{-9}$ mbar). The peaks were energy-shifted to the binding energy of Al $2p$ (74.7 eV) to correct for the charging of the material. The surface composition of the catalysts was determined from the peak areas of Pd $3d$, Bi $4f$, O $1s$, Al $2s$, and C $1s$, which were computed after subtraction of the Shirley-type background by empirically derived cross-section factors. The relative error of the analysis was $\pm 5\%$. The binding energies of Bi^{3+}/Bi^0 and Pd^{2+}/Pd^0 were determined by peak fitting. During calculation, the tabulated energy differences between Bi $4f_{7/2}$ and Bi $4f_{5/2}$ (5.39 eV) and between Pd $3d_{5/2}$ and Pd $3d_{3/2}$ (5.25 eV) were kept constant. In addition, the full width at half-maximum (FWHM) was constrained to one value. This kept the fit parameters low. Reduction of the catalyst was performed in the load lock in a similar way as described previously [51].

3. Results and discussions

3.1. Choice of catalysts and reaction conditions

On the basis of preliminary studies with various supported Pd catalysts in a batch reactor, the (oxidative) dehydrogenation of 1-phenylethanol to acetophenone was chosen as a model reaction (Scheme 1). Dehydrogenation of this aromatic alcohol was fast under mild conditions (1 bar, 55–80 °C) and the product distribution provided a sensitive test for the presence of surface hydrogen. For example, in cyclohexane at 80 °C, the selectivity to acetophenone varied between 67 and 97% in Ar depending on the catalyst and conditions, and improved up to 100% in air. In the absence of oxygen, C–O bond hydrogenolysis occurred affording ethylbenzene. As concerns the role of support material, Pd/Al_2O_3 was the most selective catalyst.

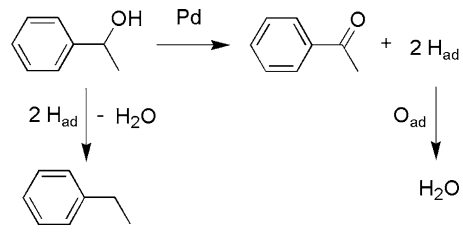

Scheme 1. Pd-catalyzed dehydrogenation of 1-phenylethanol to acetophenone and hydrogenolysis to ethylbenzene in toluene under inert and oxidative atmosphere.

Next, the conditions were optimized in the continuous-flow fixed-bed reactor cell developed for in situ EXAFS measurements. The reactor allowed relatively fast variation of the conditions such as oxygen concentration, mass flow rate, and reaction temperature, and thus reduction and oxidation of the catalyst. The reactor was mainly operated in the mass-transport-limited regime (oxygen transfer) that is a requirement for the steady operation during the aerobic oxidation of alcohols on Pt-group metals. Working in the kinetic region, where the oxygen transport to the catalyst surface is not rate limiting, results in a successive oxidation of the active sites and low reaction rates ("overoxidation") [5,8, 52]. The reactor allowed mimicking also this situation and following the changes in the oxidation state of the catalyst.

Experiments in the continuous-flow reactor revealed some catalyst deactivation during alcohol dehydrogenation in Ar. For example, under standard conditions at 80 °C, the conversion on the 5 wt% Pd/Al_2O_3 catalyst dropped from 4.3% (20 min) to 2.5–2.6% (340 min) and then stabilized at this value. We attribute this deactivation to degradation of the product acetophenone to CO and C_xH_y-type fragments. Note that there is a wealth of data evidencing decomposition of alcohols on Pt-group metals via the carbonyl compound intermediate or product [53–55]. It has been also shown that the catalyst can be (partly) regenerated by introducing oxygen [26].

3.2. Investigation of Pd/Al_2O_3 during alcohol oxidation

The oxidation state of Pd was followed by recording spectra either in the QEXAFS mode (during changes of the reaction conditions) or taking EXAFS spectra in the step scanning mode (after reaching steady state). At first (step 1, Table 2), the reactor was flushed with He-saturated toluene at 65 °C, and the spectra were recorded. The near-edge region of the Pd *K*-edge is depicted in Fig. 1a and the corresponding Fourier-transformed EXAFS spectra are shown in Fig. 1b. Spectrum 1 (start) shows that Pd was partially oxidized in the catalyst stored in air: it exhibited a white line and Pd–O scattering was observed at about 1.8 Å (Fig. 1b, not corrected for the phase shift). The small shoulder found in spectrum 1 of Fig. 1a at about 24.41 keV indicates the presence of Pd^0. In addition, Pd–Pd scattering is found in the Fourier-transformed spectrum at 2.75 Å.

Two different procedures were applied to determine the fraction of Pd^{2+}. In the case of linear combination analysis (LCA) the XANES region (24.28–24.45 keV) of the spectra was deconvoluted into Pd^{2+} and Pd^0 using the reference spectra of a PdO pellet and a Pd foil, respectively. In addition, the Fourier-filtered EXAFS spectra were fitted to those of PdO and Pd with the help of the crystallographic data summarized in Table 1. Representative fits of the Fourier-filtered EXAFS functions are shown in Fig. 2. The results of both approaches are collected in Table 2. Clearly, the untreated catalyst previously stored in air contained several outer layers of PdO. The fraction of Pd^{2+} was 0.6, as determined by LCA. The considerably oxidized state of Pd in this sample is also reflected by the coordination number (CN) and the distance to the nearest neighbors (*R*). According to these results oxygen neighbors to Pd are present and apart from the Pd–Pd distance typical for metallic Pd also the Pd–Pd distance of the second shell typical for PdO is found.

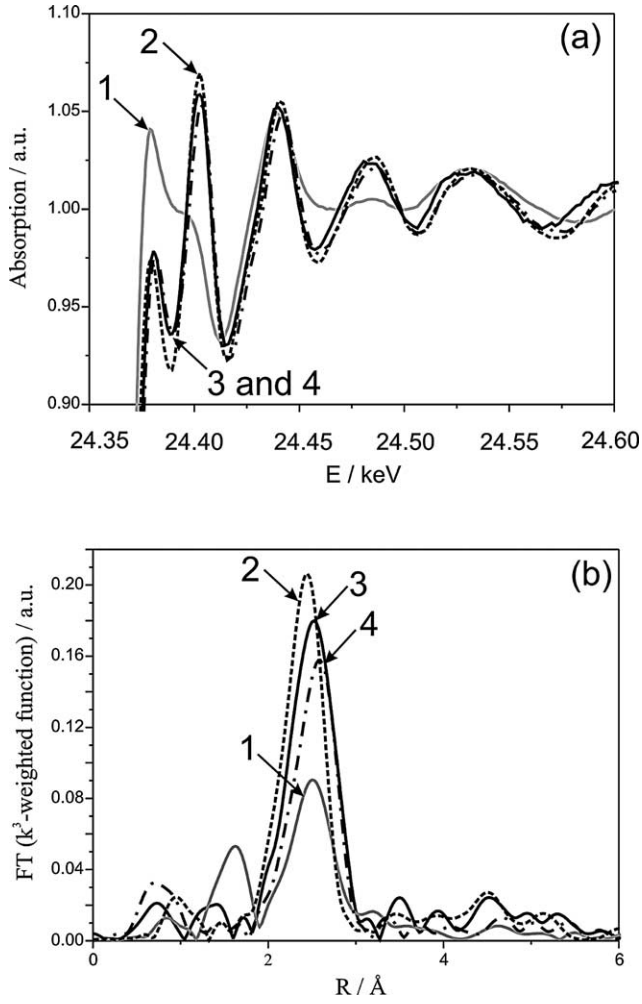

Fig. 1. Selected X-ray absorption spectra of 5 wt% Pd/Al_2O_3 at the Pd *K*-edge during the reaction series shown in Table 2: (a) normalized XANES data and (b) Fourier transform of k^3-weighted EXAFS functions (not corrected for the phase shift). The spectra were taken in He-saturated toluene at 65 °C (1), in He-saturated solution of 1-phenylethanol at 81 °C (2), in O_2-saturated toluene at 62 °C (3), and in H_2-saturated toluene at 62 °C (4).

Table 1
Crystallographic data and Fourier filtering ranges of reference compounds

Sample	Scatter atom	CN	*R* (Å)	FT range ($Å^{-1}$)
Pd foil	Pd	12	2.75	1.5–3.1
PdO	O	4	2.02	1.15–2.05
	Pd	4	3.03	2.05–3.09

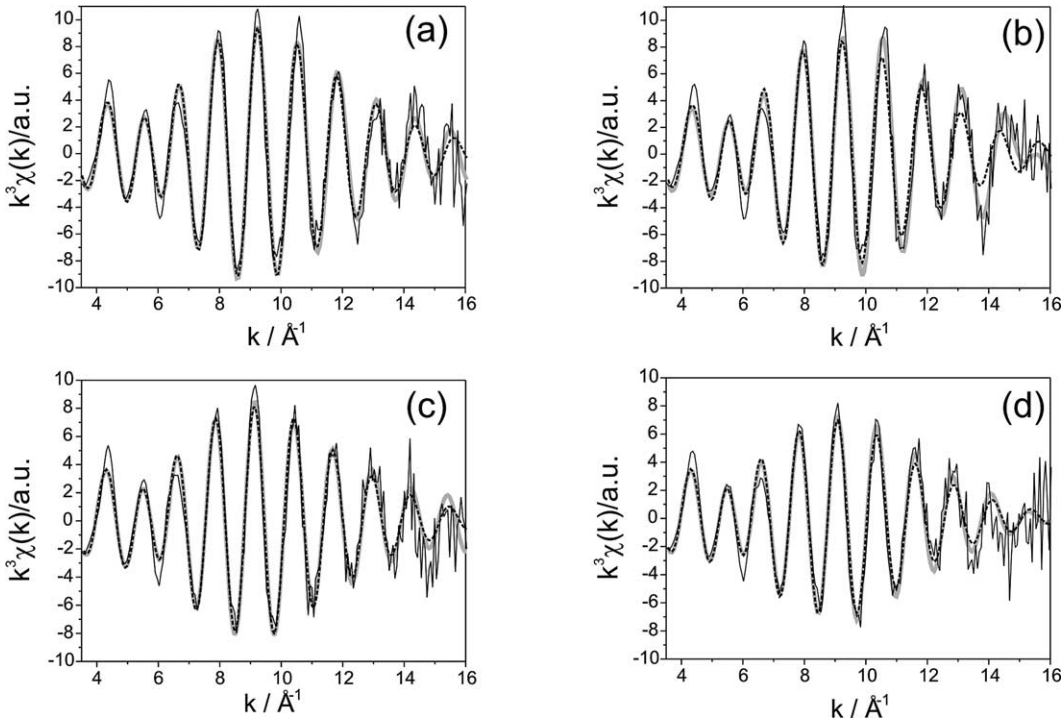

Fig. 2. Fitting of the EXAFS data of Pd/Al_2O_3 with a Pd foil and a PdO reference material. Selected k^3-weighted $\chi(k)$ functions after background removal (straight line), after extraction of the first Pd–O and Pd–Pd shells (grayish line) and the corresponding calculated fits (dashed line) are shown in (a) He-saturated solution of 1-phenylethanol at 81 °C, (b) O_2-saturated solution of 1-phenylethanol at 62 °C, (c) O_2-saturated toluene at 62 °C, and (d) H_2-saturated toluene at 62 °C. The fits were used for the data analysis presented in Table 2.

Table 2
XANES and EXAFS analysis of Pd/Al_2O_3 combined with the catalytic transformation of 1-phenylethanol in the EXAFS cell

Step in reaction series	No. of spectrum[a]	T (°C)	Atmosphere; GC sampling time	Reactant	Conversion (%)	Selectivity[b] (%)	Pd^{2+}/Pd^{0}[c]	Scatter atom	CN[c]	R (Å)	σ^2 (Å^2)	ΔE_0 (eV)
1	1	65	He	–[e]	–	–	0.60/ 0.40	O Pd Pd	2.2 3.82 2.0	2.00 2.75 3.03[d]	0.001	−0.73
2	2	81	He; After 70 min	+	3.5	78.9	0.07/ 0.93	O Pd	0.1 10.6	2.02[d] 2.76	0.0027	1.18
3	–	58	O_2; After 50 min	+	1.0	100	0.14/ 0.86	O Pd	0.2 10.2	2.02[d] 2.76	0.0031	0.08
3	–	62	O_2; After 110 min	+	< 0.1	100	0.16/ 0.84	O Pd	0.5 9.7	2.02[d] 2.76	0.0032	0.17
4	3	62	O_2	–[e]	–	–	0.18/ 0.82	O Pd	0.5 9.3	2.02[d] 2.76	0.0030	−0.62
5	4	62	H_2	–[e]	–	–	–	O Pd	0.2 10.4	1.98 2.80	0.0042	0.85

[a] The corresponding spectra are collected in Fig. 1; LCA fits were made between 24.28 and 24.45 keV using Pd foil and PdO as models (Fig. 2).
[b] Selectivity to acetophenone (see Scheme 1).
[c] Estimated error of ratio from XANES ±5%; error for EXAFS CN ±10%; for R ±1%; the goodness of fit for EXAFS [50] was about 5%.
[d] Constrained to this value during the fit.
[e] In toluene without reactant.

In step 2 (Table 2), 1-phenylethanol in He-saturated toluene was fed to the catalyst and the temperature was raised to 81 °C to accelerate the structural changes. After 30 min the catalyst was fully reduced (spectra 2 in Figs. 1a and b), and dehydrogenation of the reactant proceeded with acceptable conversion (TOF: 6.5 h^{-1}). The moderate selectivity to acetophenone was due to formation of ethylbenzene, indicating a considerable concentra-

tion of surface hydrogen necessary for the demanding C–O bond hydrogenolysis reaction. EXAFS analysis confirmed the complete reduction of Pd. Note that EXAFS detection of the reduction of Pd or Pt during alcohol dehydrogenation has already been reported [44,45]. The LCA indicated that a fraction of "only" 0.93 of Pd was present in the catalyst as Pd^0 (instead of 1.0). The difference is attributed to the fact that the near-edge structure of the X-ray absorption spectrum is not only dependent on the oxidation state and symmetry of the metal atom but it is also influenced by the size of Pd particles and the support. Thus, a Pd foil is not a perfect reference for the small Pd particles supported on a metal oxide though the relative changes in the Pd^{2+}/Pd^0 ratio can be used as additional indicator for structural changes.

In the third reaction step (Table 2) overoxidation of the catalyst was investigated, a situation in which the rate of oxygen supply is higher than the rate of alcohol oxidation, resulting in increasing oxygen coverage of the metal surface and a drop in catalytic activity [5,8]. To achieve these conditions, the feed was changed to an O_2-saturated solution of 1-phenylethanol and the temperature was decreased to around 60 °C. Table 2 shows that overoxidation of Pd was indeed achieved: the conversion of 1-phenylethanol dropped dramatically and the calculated TOF value was only 0.13 h^{-1}, compared to 6.5 h^{-1} in He at 81 °C. Partial oxidation of the Pd surface after 110 min in O_2 was evidenced by EXAFS analysis: the $CN_{Pd–Pd}$ fell to 9.7 and the fraction of Pd^{2+} increased to 0.16.

To provide a reference value for oxidized Pd under reaction conditions, the feed was changed to O_2-saturated toluene without reactant (Table 2, step 4). Omission of the reactant induced only small changes of the white line in spectrum 3 (Fig. 1a) after 45 min. The changes in the Fourier-transformed spectra were only partly visible from the increase of Pd–O scattering. The decrease of the Pd–Pd scattering was more informative: the $CN_{Pd–Pd}$ fell further to 9.3. Interestingly, the Pd^{2+} fraction determined by LCA analysis rose only to 0.18. A possible reason is the partial coverage of Pd by C_xH_y fragments produced mainly during dehydrogenation of 1-phenylethanol in He, as discussed in the former chapter.

Purging the reactor with H_2-saturated toluene for 30 min was sufficient to reduce Pd and reactivate the catalyst (Table 2, step 5). The Pd lattice expanded in the presence of hydrogen due to Pd-hydride formation, as evidenced by EXAFS analysis. Furthermore, a significant shift of spectrum 4 was observed as compared to spectrum 1 (Fig. 1b). Accordingly, removal of surface oxygen by hydrogen-saturated toluene was fast and complete.

In summary, operating the reactor in the kinetic regime led indeed to overoxidation, that is, partial coverage of the Pd surface by oxygen, which could be unambiguously confirmed by EXAFS. The observed striking drop in catalytic activity is due to the lower number of free metallic sites available for the dehydrogenation reaction [15,56].

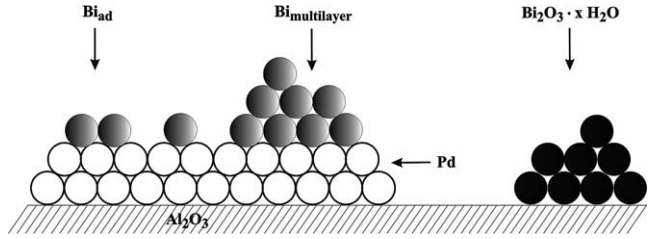

Fig. 3. Schematic representation of the structure of Bi–Pd/Al_2O_3 prepared by deposition of Bi onto Pd/Al_2O_3.

Table 3
Surface composition (at%) of the Bi–Pd/Al_2O_3 and Pd/Al_2O_3 catalysts analyzed by XPS

	Pd/Al_2O_3	Bi–Pd/Al_2O_3
C 1*s*	1.5	1.3
O 1*s*	76.8	74.9
Al 2*s*	20.9	23.0
Pd 3*d*	0.9	0.6
Bi 4*f*	–	0.2

3.3. Structure of the bimetallic catalyst

The bimetallic catalyst was prepared by consecutive reduction of Bi onto Pd/Al_2O_3. During Bi deposition, Bi adatoms (submonolayer deposition) and small Bi particles (multilayer deposition) are formed on the surface of the Pd particles. In addition, Bi^{3+}-containing particles may develop on the support, as illustrated in Fig. 3. It is expected that the promoter influences the catalytic performance of the neighboring Pd sites only. The Bi-containing particles on the support are only spectator species and the possible dissolution of Bi^{3+} in the presence of a good chelating agent reactant or product may complicate the interpretation of the promoter effect. To favor the formation of modified active sites, a special technique was applied allowing the preferential deposition of promoter metal adatoms [19,48,49]. The basis of the (nonelectrochemical) method is that under conditions where both adatom and bulk metal deposition are possible thermodynamically, formation of adatoms is kinetically favored at low Bi^{3+} concentrations. Note that the characteristics of metal adatoms has been the topic of intensive research in electrocatalysis [57,58].

XPS analysis of Pd/Al_2O_3 and Bi–Pd/Al_2O_3 (Tables 3 and 4) revealed that a considerable fraction of Pd was covered by Bi in the bimetallic catalyst as indicated by the decrease in the Pd 3*d* peak intensity. The fraction of Bi deposited onto Pd, which is reducible by hydrogen in the XPS chamber even at room temperature, was calculated to be 73%. The reduction of Bi^{3+} to Bi^0 on Pd at room temperature was confirmed also by XAS as will be discussed later. The remaining 27% Bi^{3+} is assumed to be present as $Bi_2O_3 \cdot xH_2O$ on the high surface area support (Fig. 3). Note that already during evacuating the catalyst some Bi^0 was observed by XPS that may be due to some residual hydrogen being present in the load lock. Pd^{2+} could not be detected by

Table 4
XPS analysis of Bi 4*f* and Pd 3*d* peaks in the Bi–Pd/Al_2O_3 and Pd/Al_2O_3 catalysts

	Bi^0		Bi^{3+}		Pd^0	
	Bi $4f_{7/2}$	Bi $4f_{5/2}$	Bi $4f_{7/2}$	Bi $4f_{5/2}$	Pd $3d_{5/2}$	Pd $3d_{3/2}$
Bi–Pd/Al_2O_3[a]						
Binding energy (eV)	156.9	162.3	160.7	166.1	335.4	340.6
Extent (%)[c]	33.9	29.8	16.1	20.1	54.6	45.4
FWHM (eV)	3.15	3.15	3.15	3.15	3.15	3.15
Bi–Pd/Al_2O_3[b]						
Binding energy (eV)	157.2	162.6	160.4	165.8	335.5	340.7
Extent (%)[c]	38.0	35.2	15.2	11.6	54.6	45.4
FWHM (eV)	2.95	2.95	2.95	2.95	3.0	3.0
Pd/Al_2O_3[a]						
Binding energy (eV)	–	–	–	–	335.1	340.3
Extent (%)[c]	–	–	–	–	55.2	44.8
FWHM (eV)	–	–	–	–	3.5	3.5

[a] Stored in air.
[b] After in situ reduction by hydrogen at room temperature.
[c] Estimated error ±5%.

XPS and thus Pd was in the metallic state in both Pd/Al_2O_3 and Bi–Pd/Al_2O_3.

3.4. Investigation of Bi–Pd/Al_2O_3 during alcohol oxidation

The series of (oxidative) dehydrogenation experiments carried out over Bi–Pd/Al_2O_3 is illustrated in Fig. 4. In this series we focused on the dynamic changes in the Bi constituent, since the oxidation state of Pd was already studied in the former series with Pd/Al_2O_3.

3.4.1. Step 1 (Fig. 4)

At first the Pd *K*-edge of the catalyst was probed by XAS in He-saturated toluene at 46 °C. The Pd constituent of the bimetallic catalyst stored in air (spectra 1 in Figs. 5a and b) contained less oxidized species, compared to Pd/Al_2O_3 under similar conditions (spectra 1 in Figs. 1a and b). Also the increased Pd–Pd scattering of Bi–Pd/Al_2O_3 in the Fourier-transformed EXAFS spectrum (1 in Fig. 5b) confirmed this difference. The variation is obvious when considering the preparation method: a substantial fraction of surface Pd atoms was covered by the promoter metal during deposition of Bi onto the supported Pd particles, preventing oxidation of these atoms after exposure to air. The Bi L_3-edge of the bimetallic catalyst revealed the presence of Bi^{3+} only. (This spectrum will be used as a reference for calculating the oxidation state of Bi during the subsequent reaction steps; vide infra.)

3.4.2. Step 2

Reduction of Bi–Pd/Al_2O_3 was studied by feeding a He-saturated solution of 1-phenylethanol to the catalyst (from 153 min on in Fig. 4). The temperature was raised to 65 °C to accelerate reduction of the metals. The QEXAFS spectra measured at the Bi L_3-edge are collected in Fig. 6. Reduction of Bi^{3+} started already at 46 °C and was complete within 1 h. The last QEXAFS spectrum shows that the white line around 13.44 keV (assigned to Bi^{3+}) nearly disappeared. At $t = 214$ min no further reduction of bismuth was observed and the catalyst was moderately active

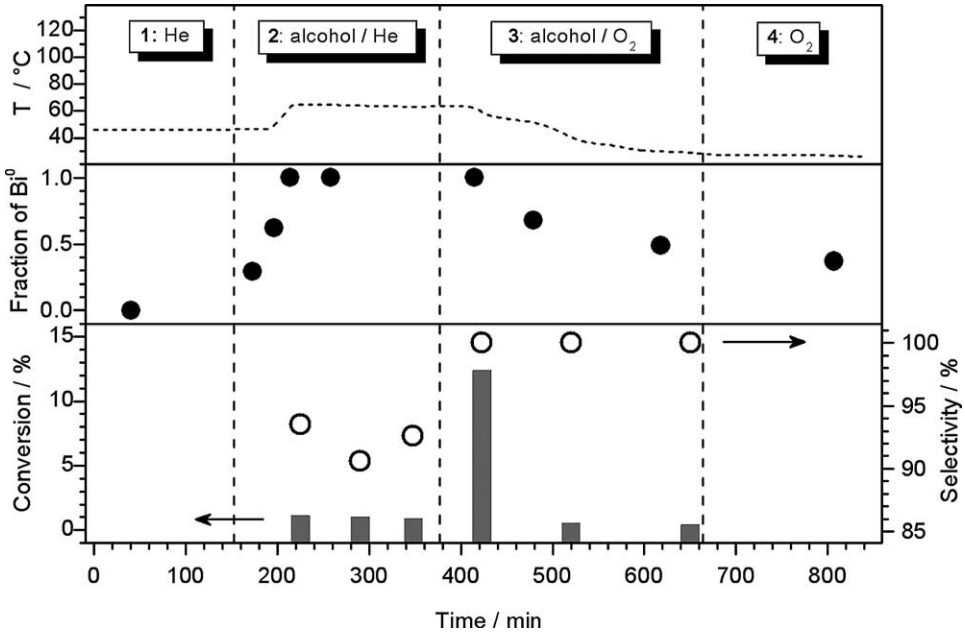

Fig. 4. Catalytic studies combined with XAS analysis during transformation of 1-phenylethanol over Bi–Pd/Al_2O_3 in the in situ EXAFS cell. Standard conditions as given in the experimental part; the only by-product is ethylbenzene. Vertical dashed lines indicate the change of the feed composition; toluene was always present in the feed.

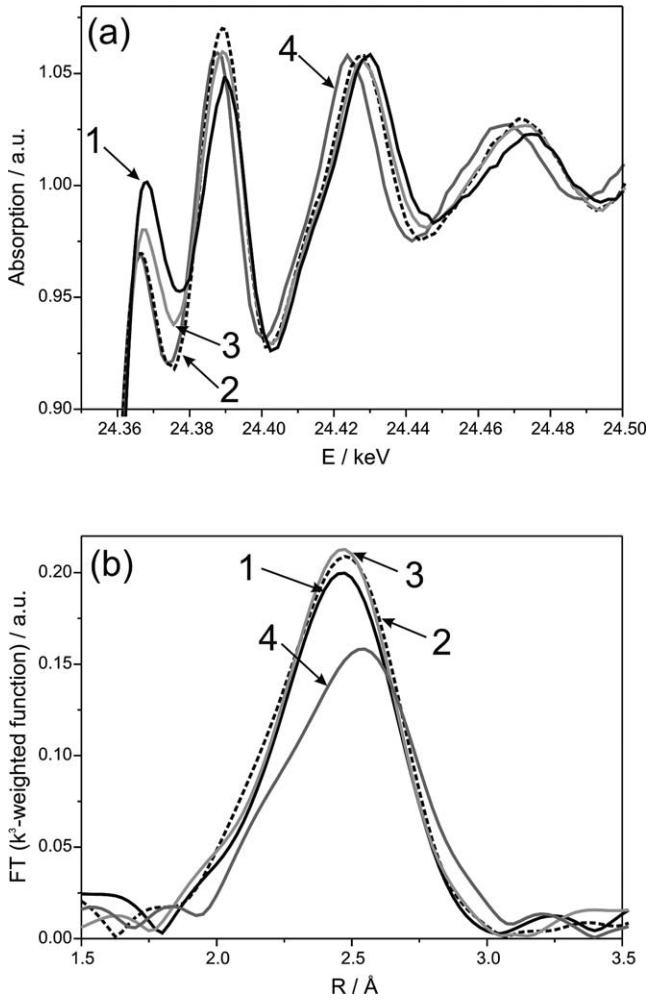

Fig. 5. Selected X-ray absorption spectra of Bi–Pd/Al_2O_3 at the Pd K-edge during the reaction series shown in Fig. 4: (a) normalized XANES spectra and (b) Fourier-transformed k^3-weighted EXAFS functions. The spectra were taken in He-saturated toluene at 46 °C (1), in He-saturated solution of 1-phenylethanol at 62 °C (2), in O_2-saturated toluene at 27 °C (3), and in H_2-saturated toluene at 82 °C (4).

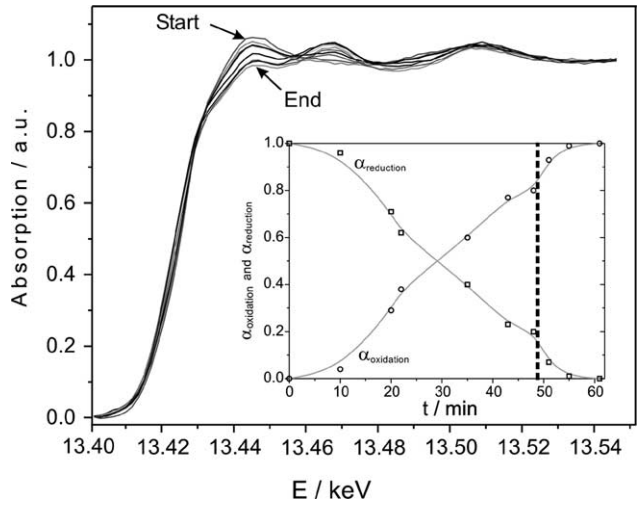

Fig. 6. QEXAFS spectra at the Bi L_3-edge of Bi–Pd/Al_2O_3 recorded in a He-saturated toluenic solution of 1-phenylethanol at 46 °C (step 2 in Fig. 4). The inset shows the extent (α) of reduced and oxidized Bi determined by linear combination of the first and last QEXAFS spectrum. At the dotted line (48 min) the temperature was raised to 65 °C.

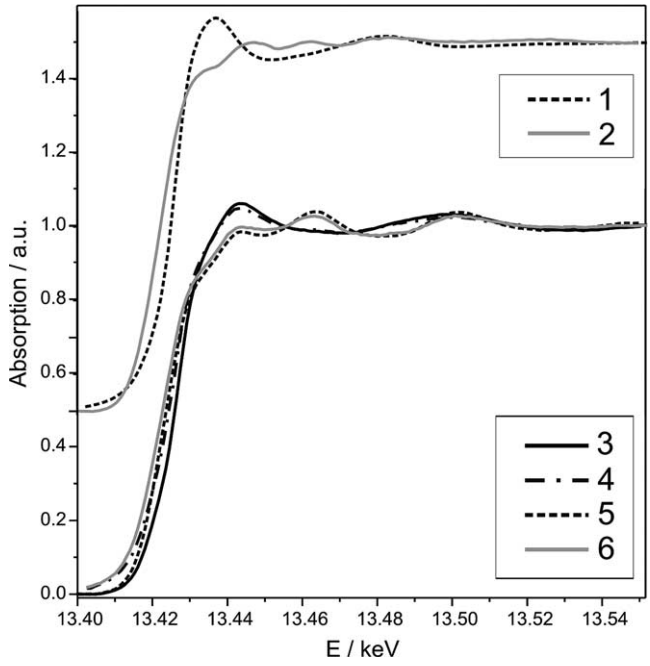

Fig. 7. XANES spectra at the Bi L_3-edge of Bi–Pd/Al_2O_3 compared to reference materials. (1) $Bi(NO_3)_3 \cdot 5H_2O$; (2) Bi metal powder; (3) Bi–Pd/Al_2O_3 catalyst in air before reduction (no solvent); (4) Bi–Pd/Al_2O_3 catalyst in He-saturated toluene (step 1 in Fig. 4); (5) Bi–Pd/Al_2O_3 catalyst after reduction by 5% H_2 in Ar at 35 °C (no solvent); (6) Bi–Pd/Al_2O_3 catalyst reduced by 1-phenylethanol in He-saturated toluene at 84 °C (not shown in Fig. 4).

in 1-phenylethanol dehydrogenation (Fig. 4). The product distribution (93% selectivity to acetophenone and 7% selectivity to ethylbenzene) reflects the presence of considerable amount of hydrogen on the surface Pd sites necessary for the hydrogenolysis of the C–O bond (Scheme 1).

Fig. 7 illustrates that the XANES spectra of the catalyst stored in air (measured as a pellet, spectrum 3) and after its exposure to He-saturated toluene (measured as a powder, spectrum 4) are very similar. The white line at 13.44 keV is also found in $Bi(NO_3)_3$ and is typical for Bi^{3+}, while it is decreased for the Bi metal powder and also the reduced Bi–Pd/Al_2O_3 catalyst. In addition, the spectrum taken after reduction by diluted gaseous H_2 (spectrum 5) and that recorded after reduction by 1-phenylethanol in He-saturated toluene (spectrum 6) are almost identical. Reduction in the absence of solvent by 5% H_2 in Ar at 200 °C (not shown here) and at room temperature (spectrum 5) indicated the same extent of reducible Bi. In conclusion, 1-phenylethanol reduces the Bi promoter in Bi–Pd/Al_2O_3 to about the same extent as diluted gaseous H_2. Accordingly, the fraction of Bi^0 in Fig. 4 was calculated by linear combination of the spectra of "oxidized" and "reduced" Bi–Pd/Al_2O_3 (Fig. 7,

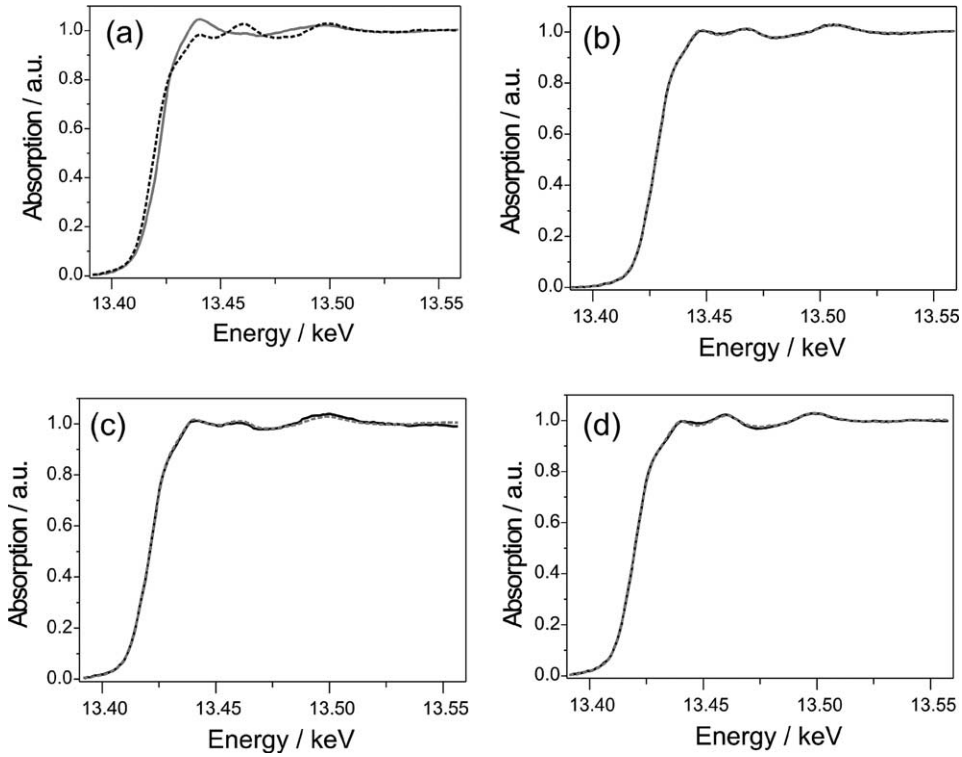

Fig. 8. Selected Bi L_3-XANES spectra of Bi–Pd/Al_2O_3 and the resulting fits achieved by linear combination analysis (LCA). (a) Reference spectra for LCA (oxidized, straight line; reduced, dashed line), (b) He-saturated solution of 1-phenylethanol at 47 °C ($t = 196$ min in Fig. 4; measured spectrum, straight line; corresponding fit, dashed line), (c) O_2-saturated solution of 1-phenylethanol at 30 °C ($t = 618$ min in Fig. 4; measured spectrum, straight line), (d) H_2-saturated toluene at 82 °C (measured spectrum, straight line; spectrum 7 in Fig. 9). The calculated fraction of Bi^0 is shown in Fig. 4.

spectra 4 and 6). Some selected fits obtained from linear combination of the reference spectra are shown in Fig. 8. The LCA fits were performed in the near-edge region (13.37–13.56 keV). The QEXAFS data shown in Fig. 6 were also analyzed by LCA using the starting and final scan (interval 13.41–13.55 keV).

The original XANES spectra at the Bi L_3-edge of Bi–Pd/Al_2O_3, taken during the continuous experiment in Fig. 4, are shown in Fig. 9. The pronounced difference between spectra 1 and 2 is due to reduction by 1-phenylethanol in the absence of oxygen. As noted before, spectrum 2 refers to the state of the catalyst where all reducible Bi is present as Bi^0. The small white line at 13.44 keV compared to Bi powder (spectrum 2 in Fig. 7) may be due to some Bi present as Bi^{3+} (presumably $Bi_2O_3 \cdot xH_2O$) on the support. These species are not reducible by hydrogen even at 200 °C. Note that XPS confirmed this interpretation, as discussed above. An important conclusion from Fig. 9 is that reduction of the bimetallic catalyst at 82–84 °C by hydrogen-saturated toluene (spectrum 7) or by 1-phenylethanol in toluene (spectrum 6) affords almost identical oxidation states of Bi.

After reduction of Bi–Pd/Al_2O_3 by 1-phenylethanol, the crystal was changed from Si(111) to Si(311) and the Pd constituent was analyzed at the Pd K-edge. Spectra 2 in Fig. 5 show that also Pd was reduced during dehydrogenation of 1-phenylethanol in He, as expected.

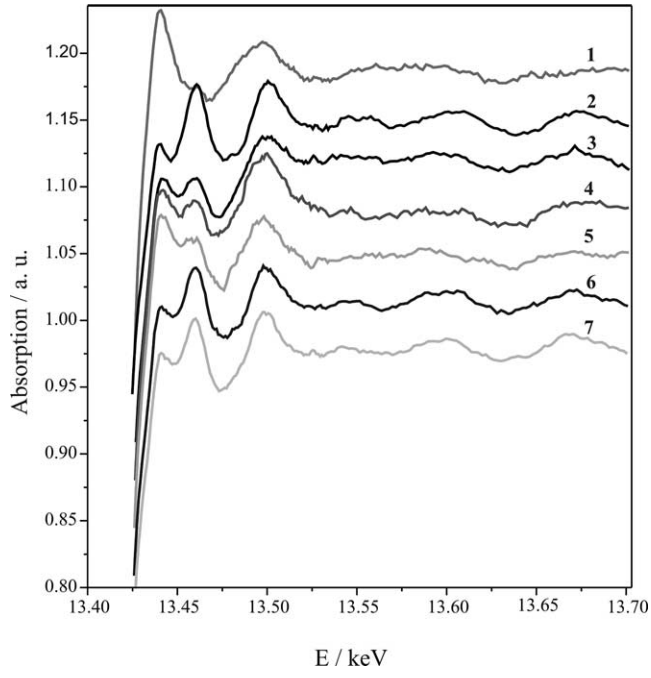

Fig. 9. XANES spectra at the Bi L_3-edge of Bi–Pd/Al_2O_3. (1) In He-saturated toluene at 46 °C (step 1 in Fig. 4); (2) in He-saturated solution of 1-phenylethanol at 64 °C (step 2 in Fig. 4); (3) in O_2-saturated solution of 1-phenylethanol at 48 °C (step 3 in Fig. 4); (4) the same as (3) but at 30 °C; (5) in O_2-saturated toluene at 27 °C (step 4 in Fig. 4); (6) in He-saturated solution of 1-phenylethanol at 84 °C (not included in Fig. 4); (7) in H_2-saturated toluene at 82 °C (not included in Fig. 4).

3.4.3. Step 3

Alcohol oxidation and reoxidation of the bimetallic catalyst was investigated stepwise by changing the feed from He- to O_2-containing toluenic solution of 1-phenylethanol (Fig. 4). Addition of molecular oxygen resulted in a rate enhancement by a factor of 12. Besides, the by-product ethylbenzene disappeared, indicating that the actual hydrogen concentration on the Pd sites was negligible. Still, the oxidation state of Bi did not change detectably ($t = 415$ min), despite the presence of oxygen in the feed. These conditions seem to be ideal for the oxidation of 1-phenylethanol: the reaction runs fast and selective over a completely reduced metal surface. Assuming a solution saturated with O_2 at the reaction temperature [59], the theoretical limit of alcohol conversion was higher than 80%.

Next, we tried to mimic the so-called overoxidation of the catalyst by applying the same feed and decreasing the reactor temperature. The phenomenon is well known in the literature and is based on the fact that the dehydrogenation activity of oxidized Pd or Pt is remarkably lower than that of the reduced metal surface [15,56]. Lowering the temperature diminished the rate of alcohol dehydrogenation and increased the solubility of oxygen in the feed. Induced by these two effects, the rate of oxygen supply to the catalyst surface successively exceeded the rate of alcohol dehydrogenation, the bimetallic particles were oxidized, and the rate of alcohol dehydrogenation dropped further to a low value ($t = 520$ min, Fig. 4). Spectra 3 and 4 in Fig. 9 show that reoxidation of Bi during catalyst overoxidation was incomplete. A prolonged exposure of the catalyst to these conditions increased the fraction of Bi^{3+}, though complete reoxidation of the promoter metal was not achieved ($t = 618$ min, Fig. 4). Interestingly, further oxidation of the Bi constituent was not reflected by any change in the catalytic properties (conversion and selectivity, Fig. 4).

3.4.4. Step 4

The oxidation state of Bi was further investigated in the absence of 1-phenylethanol. As spectrum 5 in Fig. 9 shows, complete reoxidation of Bi could not be achieved even after exposure to oxygen-saturated toluene for several hours at room temperature. LCA revealed a fraction of 63% Bi^{3+} at 807 min time on stream (Fig. 4). Assuming again that the feed was saturated with O_2 [59], we calculated that complete oxidation of the total amount of surface Pd, and Bi atoms on the Pd particles, would require less than 30 s.

A plausible explanation for the incomplete reoxidation of Bi is that the surface Bi atoms were partially covered by a strongly (irreversibly) adsorbed organic residue. As noted above, preliminary studies in the continuous-flow reactor cell indicated a significant catalyst deactivation, which we attributed to product degradation to CO and C_xH_y-type fragments. Oxidation of these poisoning species is incomplete at close to ambient temperature. In a control experiment we tried to regenerate the catalyst by reduction with the He-saturated solution of 1-phenylethanol at 84 °C. The reduction of Bi^{3+} by the alcohol occurred fast but remained incomplete (fraction of $Bi^0 = 0.83$). A comparison of spectra 2 to 6 in Fig. 9 reveals that the intensity differences between the second and the first maximum in spectrum 6 is lower, indicating a lower fraction of reduced Bi. This difference corroborates the assumption that a part of the bimetallic catalyst is successively covered by organic residue during the long experiment, the contamination of which distorts the structural analysis.

Parallel to the analysis of the Bi constituent, the oxidation state of Pd in Bi–Pd/Al_2O_3 was also investigated in oxygen-saturated toluene. Spectra 3 in Figs. 5a and b reveal only a partial reoxidation of Pd. The deviation at the Pd K-edge is smaller than that observed for Pd/Al_2O_3 (spectra 3, Figs. 1a and b). The reason for this difference is the structure of the bimetallic catalyst: a large fraction of surface Pd atoms is covered by Bi. Note that a reference spectrum for completely reduced Pd in Bi–Pd/Al_2O_3 cannot be obtained by feeding H_2-saturated toluene due to hydride formation (spectrum 4, Fig. 5).

From the point of view of alcohol oxidation with molecular oxygen, the most interesting observation is the reduced state of both metal components in Bi–Pd/Al_2O_3 during reaction (step 3, at ca. 420 min in Fig. 4). This result was confirmed in another study [46], which was carried out under standard conditions in a similar way as depicted in Fig. 4 but 65 mg catalyst was filled in the reactor instead of 28 mg. The reactor temperature was kept constant at 60 °C throughout the procedure. The conditions for aerobic oxidation were maintained for more than 2 h by feeding air-saturated toluenic solution of 1-phenylethanol. During that period both the Pd K-edge and the Bi L_3-edge were analyzed. The analysis corroborated that both Bi and Pd remained in a reduced state, despite the presence of oxygen.

3.5. Advantages and limitations of in situ XAS for structural analysis of unpromoted and promoted Pd/Al_2O_3

In situ XAS studies over Pd/Al_2O_3 and Bi–Pd/Al_2O_3 have shown that the structural transformations (oxidation/reduction) during variation of the alcohol/oxygen ratio are similar for both the Pd and the Bi constituent. However, the structural changes are more pronounced at the Bi L_3-edge. This is due to the location of Bi on the surface of the Pd particles and according to XPS only a fraction of 27% is present on the support as "spectator species" (denoted here as species that are not involved in the redox reaction of the metals; see $Bi_2O_3 \cdot xH_2O$ in Fig. 3). The fact that Bi stays on the surface is supported by XPS and previous experimental evidence for Bi on noble metal surfaces [60]. This is the main reason for improved surface sensitivity compared to the Pd constituent, where the major part reflects "bulk species" (which are not involved in redox processes at the surface). Surface sensitivity in EXAFS studies is usually improved by higher metal dispersion in case of small metal particles, particularly reported for gas-phase reactions

[61,62]. Surface sensitivity was also enhanced for in situ XAS studies by deposition of a thin active catalyst layer on top of an inert metal oxide support, i.e., a V–P–O layer on top of SiO_2 [63]. With respect to the Pd/Al_2O_3 catalyst this would mean that palladium is used in a high dispersion. This may, however, also lead to a different catalytic performance and/or sintering effects during the dynamic changes of the reaction atmosphere.

Hence, not only the study of a promoter atom itself is interesting but also another attractive strategy is the use of a promoter atom as "probe atom" instead of special layer-type model catalysts. In the present study the number of "spectator species" could be reduced to a low level by the special deposition technique, which preferentially deposited the Bi atoms onto the surface of the Pd particles. In general, the probing of promoter atoms or bimetallic catalysts with one of the components being located on the surface may be an alternative to the usually applied procedure of using thin layers of the active catalyst species or high metal dispersion to increase the surface sensitivity of XAS. However, the model system must be carefully chosen because surface sensitivity is not enhanced if the deposited metal atoms segregate into the metal particle or promoter atoms diffuse into the metal oxide support. For Bi and Pb as promoter atoms on top of Pd the tendency to form surface adatoms is high [57]. The investigation of Pt on top of Pd is less useful since Pt has the tendency to segregate into the Pd particle [64,65] and Pt and Pd form mixed alloys.

Using the $Bi–Pd/Al_2O_3$ system allowed us to study the catalyst element specific under reaction conditions. Although the number of spectator species could be minimized by studying Bi adatoms, such studies under real catalytic conditions are also often disturbed by surface impurities, formed during reaction. These impurities led not only to decrease of the catalytic activity but also to an increase of the number of metal atoms that are not involved in the reaction any more (spectator species due to the fact that they are covered by impurities) and thus disturb the spectroscopic measurements.

Presently, XAS is probably the most appropriate method for monitoring dynamic structural changes in the oxidation state of metals during a catalytic reaction in a nonconductive organic medium.

3.6. Implications to the mechanism of alcohol oxidation on Bi-promoted Pd

It is generally accepted that promotion of Pt-group metals by Bi, Pb, or other inactive components can improve the activity and selectivity in alcohol oxidation with molecular oxygen [2,5–9]. Several methods have been developed for the fine tuning of the structure of the bimetallic catalysts and the improvements achieved are sometimes dramatic. There is no agreement, however, in the mechanistic understanding of the role of promoters. Many plausible models have been suggested in the past years, which are supported only by indirect observations, such as kinetic analysis. The present study provides unambiguous evidence for the reduced, metallic state of Pd and Bi in Bi-promoted Pd/Al_2O_3 during the oxidation of 1-phenylethanol to acetophenone. Clearly, on the surface of the particles the oxidation state of both metals is the same during dehydrogenation in Ar and during oxidation with molecular oxygen. Among the various models referred to in the Introduction, the geometric blocking of a fraction of active sites by the modifier fits best to these observations [16,17]. This model assumes that the major role of modifier is the suppression of side reactions by decreasing the size of Pd active site ensembles. In line with this model, a recent ATR-IR study on the oxidation of cinnamyl alcohol over Pd/Al_2O_3 indicated that the reaction obeyed a dehydrogenation mechanism and the major role of oxygen was the removal of poisoning species (CO and C_xH_y fragments) from the active sites [26].

Another model that conforms with the reduced state of promoter during alcohol oxidation assumes the presence of intermetallic compounds [20–22], in our case Bi_2Pd and BiPd [21], as active sites. However, formation of intermetallic compounds requires elevated temperatures and our catalysts were prepared under very mild conditions, at room temperature. Hence, this possibility is unlikely.

A further important conclusion is that the promoter effect in alcohol oxidation is a truly heterogeneous catalytic phenomenon. As both metals were in a reduced state during oxidation, dissolution of bismuth as Bi^{3+} and homogeneous catalysis can be excluded.

Measurement of catalyst potential during oxidation of alcohols and polyols [25,26] has revealed that in some cases, for example, in sorbose oxidation [66], the reactions ran only on a partially oxygen-covered metal surface; partially hydrogen-covered metal was inactive. Clearly, the structure of the reactant and product has a critical influence on the side reactions and may also affect the oxidation state of the catalyst during reaction. It remains the task of future work to clarify to which extent the observations presented here can be generalized to other reactions and other bimetallic catalysts.

4. Conclusions

Catalytic oxidation and dehydrogenation of an aromatic alcohol in an organic medium were performed in a continuous-flow fixed-bed reactor. The reactor was designed to serve at the same time as an EXAFS cell and the oxidation state of the supported metal catalyst was followed in situ by XANES/EXAFS spectroscopy. This approach provides insight into the structure-activity relationship at the solid/liquid interphase, similarly to previous in situ studies of gas/solid-type reactions [32–35]. An important feature of our approach is that the Bi promoter was present mainly on the Pd surface. This structure resulted in high Bi dispersion and the "bulk technique" XAS could sensitively detect the

changes in the oxidation state of the promoter atom. This technique of using "probe atoms" may be generally applicable for in situ catalytic studies. A considerable advantage of using XANES/EXAFS is that the technique is not sensitive to the reaction medium and it is element specific, in contrast to IR spectroscopy or catalyst potential measurement.

Dynamic changes in the activity and selectivity of a Pd/Al_2O_3 and a Bi-promoted Pd/Al_2O_3 catalyst were detected during the transformation of 1-phenylethanol in toluene, induced by the changes in the actual surface concentration of oxygen. XANES/EXAFS spectroscopy revealed that both the promoter metal (Bi) and the active noble metal component (Pd) were in a reduced state in the presence of oxygen when the reaction ran with a high rate and 100% selectivity to acetophenone. This observation conforms with the classical dehydrogenation mechanism of alcohol oxidation on Pt-group metals, namely that the reaction proceeds via dehydrogenation and the coproduct hydrogen is oxidized to water. The reduced state of the noble metal is due to the presence of surface hydrogen and the alcohol/carbonyl compound redox couple.

The present results allow us to extend this model to bimetallic catalysts. There are several contradictory explanations for the positive effect of promoter metals on the rate and selectivity of alcohol oxidation over Pt-group metals. None of these models, addressed in the Introduction, has been supported yet with in situ analysis of the oxidation state of the promoter metal. The present study indicates that only those models can be used to rationalize the promoter effect that do not assume a partially or completely oxidized state of the promoter metal.

Notation

E	Photoelectron energy (keV)
ΔE_0	Difference in the origin of photoelectron energy between the reference and the sample (eV)
CN	Coordination number of nearest neighbors of a central atom, calculated from the EXAFS fit
R	Bond length to the corresponding neighbors (Å)
σ^2	Debye–Waller factor (Å^2)
k	Wave vector of a photoelectron
$\chi(k)$	Normalized EXAFS function
μ	Absorption coefficient
FWHM	Full width at half-maximum
LCA	Linear combination analysis

Acknowledgments

The authors thank HASYLAB for offering beam time and ETH Zurich for financial support. The beamline staff at beamline X1, as well as M. Caravati, S. Hannemann, and M. Ramin, are acknowledged for the support during the measurements. Thanks are also due to P. Trüssel (LTC, mechanical workshop) and M. Wohlwend (LTC, electronic workshop) for their valuable support in the design of the in situ setup. In addition, we are grateful to Dr. F. Krumeich for TEM measurements.

References

[1] A.H. Haines, Methods for the Oxidation of Organic Compounds, Academic Press, London, 1988.
[2] H. van Bekkum, in: F.W. Lichtenthaler (Ed.), Carbohydrates as Organic Raw Materials, VCH, Weinheim, 1991, p. 289.
[3] H. Röper, in: F.W. Lichtenthaler (Ed.), Carbohydrates as Organic Raw Materials, VCH, Weinheim, 1991, p. 267.
[4] P. Vinke, D. de Wit, A.T.J.W. de Goede, H. van Bekkum, Stud. Surf. Sci. Catal. 72 (1992) 1.
[5] T. Mallat, A. Baiker, Catal. Today 19 (1994) 247.
[6] P. Gallezot, Catal. Today 37 (1997) 405.
[7] M. Besson, P. Gallezot, Catal. Today 57 (2000) 127.
[8] J.H.J. Kluytmans, A.P. Markusse, B.F.M. Kuster, G.B. Marin, J.C. Schouten, Catal. Today 57 (2000) 143.
[9] M. Besson, P. Gallezot, in: R.A. Sheldon, H. van Bekkum (Eds.), Fine Chemicals through Heterogeneous Catalysis, Wiley–VCH, Weinheim, 2001, p. 507.
[10] H. Lefranc, European patent 0,667,331 B1, 1999.
[11] T. Mallat, Z. Bodnar, A. Baiker, Stud. Surf. Sci. Catal. 78 (1993) 377.
[12] P.C.C. Smits, B.F.M. Kuster, K. van der Wiele, H.S. van der Baan, Carbohydr. Res. 153 (1986) 227.
[13] H. Kimura, A. Kimura, I. Kokubo, T. Wakisaka, Y. Mitsuda, Appl. Catal. A 95 (1993) 143.
[14] P.C.C. Smits, B.F.M. Kuster, K. van der Wiele, H.S. van der Baan, Appl. Catal. 33 (1987) 83.
[15] M. Besson, P. Gallezot, in: R.A. Sheldon, H. van Bekkum (Eds.), Fine Chemicals through Heterogeneous Catalysis, Wiley–VCH, Weinheim, 2001, p. 491.
[16] T. Mallat, A. Baiker, J. Patscheider, Appl. Catal. A 79 (1991) 59.
[17] H. Kimura, K. Tsuto, T. Wakisaka, Y. Kazumi, Y. Inaya, Appl. Catal. A 96 (1993) 217.
[18] R. Parsons, T. VanderNoot, J. Electroanal. Chem. 257 (1988) 9.
[19] T. Mallat, Z. Bodnar, A. Baiker, O. Greis, H. Strübig, A. Reller, J. Catal. 142 (1993) 237.
[20] T. Tsujino, S. Ohigashi, S. Sugiyama, K. Kawashiro, H. Hayashi, J. Mol. Catal. 71 (1992) 25.
[21] M. Wenkin, C. Renard, P. Ruiz, B. Delmon, M. Devillers, Stud. Surf. Sci. Catal. 108 (1997) 391.
[22] S. Karski, I. Witonska, J. Mol. Catal. A 191 (2003) 87.
[23] M. Wenkin, P. Ruiz, B. Delmon, M. Devillers, J. Mol. Catal. A 180 (2002) 141.
[24] H. Topsøe, Stud. Surf. Sci. Catal. 130 (2000) 1.
[25] D. Ferri, T. Bürgi, A. Baiker, J. Phys. Chem. B 105 (2001) 3187.
[26] C. Keresszegi, T. Bürgi, T. Mallat, A. Baiker, J. Catal. 211 (2002) 244.
[27] R. DiCosimo, G.M. Whitesides, J. Phys. Chem. 93 (1989) 768.
[28] T. Mallat, A. Baiker, Catal. Today 24 (1995) 143.
[29] A.P. Markusse, B.F.M. Kuster, J.C. Schouten, Catal. Today 66 (2001) 191.
[30] C. Wagner, W. Traud, Z. Electrochem. Angew. Phys. Chem. 44 (1938) 52.
[31] M. Spiro, Catal. Today 17 (1993) 517.
[32] B.S. Clausen, H. Topsøe, R. Frahm, Adv. Catal. 42 (1998) 315.
[33] J.-D. Grunwaldt, B.S. Clausen, Top. Catal. 18 (2002) 37.
[34] M. Fernandez-Garcia, Catal. Rev.-Sci. Eng. 44 (2002) 59.
[35] D. Bazin, H. Dexpert, J. Lynch, in: Y. Iwasawa (Ed.), X-Ray Absorption Fine Structure for Catalysts and Surfaces, World Scientific, Singapore, 1996, p. 113.
[36] M. Vaarkamp, J.T. Miller, F.S. Modica, D.C. Koningsberger, J. Catal. 163 (1996) 294.
[37] G. Sankar, J.M. Thomas, Top. Catal. 8 (1999) 1.

[38] R. Frahm, Phys. B 158 (1989) 342.
[39] J.D. Grunwaldt, D. Lützenkirchen-Hecht, M. Richwin, S. Grundmann, B.S. Clausen, R. Frahm, J. Phys. Chem. B 105 (2001) 5161.
[40] M. Hagelstein, S. Cunis, R. Frahm, W. Niemann, P. Rabe, Phys. B 158 (1989) 324.
[41] A.J. Dent, Top. Catal. 18 (2002) 27.
[42] G. Sankar, J.M. Thomas, R.A. Catlow, Top. Catal. 10 (2000) 255.
[43] H.H.C.M. Pinxt, B.F.M. Kuster, D.C. Koningsberger, G.B. Marin, Catal. Today 39 (1998) 351.
[44] A.P. Markusse, B.F.M. Kuster, D.C. Koningsberger, G.B. Marin, Catal. Lett. 55 (1998) 141.
[45] J.-D. Grunwaldt, C. Keresszegi, T. Mallat, A. Baiker, J. Catal. 213 (2003) 291.
[46] C. Keresszegi, J.-D. Grunwaldt, T. Mallat, A. Baiker, Chem. Commun. 18 (2003) 2304.
[47] A. Borodzinski, M. Bonarowska, Langmuir 13 (1997) 5613.
[48] C. Brönnimann, Z. Bodnar, P. Hug, T. Mallat, A. Baiker, J. Catal. 150 (1994) 199.
[49] T. Mallat, Z. Bodnar, P. Hug, A. Baiker, J. Catal. 153 (1995) 131.
[50] T. Ressler, J. Synchrotron Rad. 5 (1998) 118.
[51] J.D. Grunwaldt, M.D. Wildberger, T. Mallat, A. Baiker, J. Catal. 177 (1998) 53.
[52] H.E. van Dam, A.P.G. Kieboom, H. van Bekkum, Appl. Catal. 33 (1987) 361.
[53] B.J. Wood, H. Niki, H. Wise, J. Catal. 26 (1972) 465.
[54] J.L. Davis, M.A. Barteau, Surf. Sci. 187 (1987) 387.
[55] R.M. Souto, J.L. Rodriguez, E. Pastor, T. Iwasita, Langmuir 16 (2000) 8456.
[56] P.J.M. Dijkgraaf, M.J.M. Rijk, J. Meuldijk, K. van der Wiele, J. Catal. 112 (1988) 329.
[57] E. Herrero, L.J. Buller, H.D. Abruna, Chem. Rev. 101 (2001) 1897.
[58] S. Szabo, Int. Rev. Phys. Chem. 10 (1991) 207.
[59] R. Battino, H.L. Clever, C.L. Young, in: R. Battino (Ed.), Oxygen and Ozone, Pergamon, Oxford, 1981, p. 257.
[60] M. Ball, C.A. Lucas, N.M. Markovic, B.M. Murphy, P. Steadman, T.J. Schmidt, V. Stamenkovic, P.N. Ross, Langmuir 17 (2001) 5943.
[61] B.S. Clausen, J. Schiotz, L. Grabek, C.V. Ovesen, K.W. Jacobsen, J.K. Norskov, H. Topsøe, Top. Catal. 1 (1994) 367.
[62] J.D. Grunwaldt, A.M. Molenbroek, N.Y. Topsøe, H. Topsøe, B.S. Clausen, J. Catal. 194 (2000) 452.
[63] G.W. Coulston, S.R. Bare, H. Kung, K. Birkeland, G.K. Bethke, R. Harlow, N. Herron, P.L. Lee, Science 275 (1997) 191.
[64] A.V. Ruban, H.L. Skriver, J.K. Norskov, Phys. Rev. B 59 (1999) 15990.
[65] E. Christoffersen, P. Liu, A. Ruban, H.L. Skriver, J.K. Norskov, J. Catal. 199 (2001) 123.
[66] C. Brönnimann, Z. Bodnar, R. Aeschimann, T. Mallat, A. Baiker, J. Catal. 161 (1996) 720.